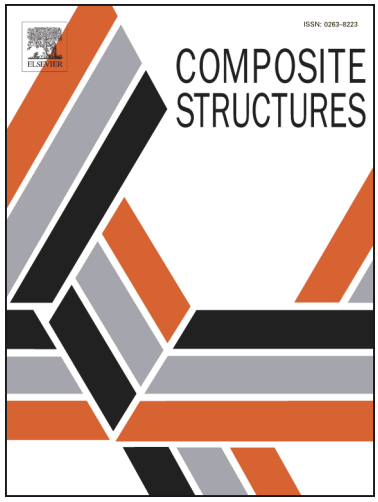

Damage detection of sandwich panels with truss core based on time domain dynamic responses

Lingling Lu, Jie Le, Hongwei Song, Yabo Wang, Chenguang Huang

PII: S0263-8223(18)32570-4
DOI: https://doi.org/10.1016/j.compstruct.2018.12.052
Reference: COST 10515

To appear in: *Composite Structures*

Received Date: 24 July 2018
Accepted Date: 20 December 2018

Please cite this article as: Lu, L., Le, J., Song, H., Wang, Y., Huang, C., Damage detection of sandwich panels with truss core based on time domain dynamic responses, *Composite Structures* (2018), doi: https://doi.org/10.1016/j.compstruct.2018.12.052

Damage detection of sandwich panels with truss core based on time domain dynamic responses

Lingling LU[1,2], Jie LE[3], Hongwei SONG[1,2*], Yabo WANG[1,2], Chenguang HUANG[1,2]

[1] Key Laboratory for Mechanics in Fluid Solid Coupling Systems, Institute of Mechanics, Chinese Academy of Sciences, Beijing China, 100190

[2] School of Engineering Science, University of Chinese Academy of Sciences, Beijing, China, 100049

[3] College of Mechanical and Electrical Engineering, Harbin Engineering University, Harbin, China, 150001

Abstract A damage identification method, based on structural time domain dynamic responses and Teager energy operator, is presented for sandwich panels with truss core in the paper. The dimensionless structural dynamic responses, i.e., dimensionless velocity and displacement, are combined to construct damage index. Application of the method on sandwich panels in the cases of single damage and multiple damages with different extents are conducted. Effects of some factors on the method are discussed, including excitation location, excitation frequency, boundary condition, number of points *N* in Poincare maps. Numerical and experimental results show that the proposed method is effective in detecting both single damage and multiple damages with different extents. Excitation location plays a very important role in affecting the effectiveness of the method. Excitation frequency has little effect on the method, and there is a great selection space of excitation frequencies. Increasing the boundary condition constraint is beneficial for damage identification.

Keywords Sandwich panel with truss core, Damage identification, Dimensionless time domain dynamic response, Teager energy operator, Poincare map

*Corresponding author, Tel.: +8610 82544149; E-mail address: songhw@imech.ac.cn (H.W. Song)

1. Introduction

Sandwich panels with truss core (SPTCs), a class of newly developed lightweight multifunctional structures, possess superior properties such as high specific bending stiffness, excellent shock resistance, good thermal insulation and acoustical isolation [1-4]. Compared with conventional structures, like beams and plates, it is more difficult to identify damages of SPTCs. On the one hand, damage styles in SPTCs are diverse, including buckling of the panel [5, 6], breakage of truss, burn-through of face sheets, unbounded truss nodes to the face sheet, etc. On the other hand, the identification of inner damages (like unbound nodes, truss core missing) needs more effective and sensitive damage indexes, compared with the identification of surface damages.

In recent 20 years, vibration-based structural health monitoring (VSHM) methods are quite popular and extensively used in monitoring structures and damage identification [7]. VSHM is based on the fact that any changes introduced into a structure result in changes in stiffness, mass or energy dissipation. Therefore, many previous studies on VSHM were based on changes in the dynamic characters of structures, such as natural frequencies, vibration modes, modal curvature [8-11].

For sandwich structures, some works have been reported on vibration-based damage detection. For composite laminates, Hu et al [12] used strain energy method to detect surface cracks. For composite sandwich beam, Kumar et al [13] proposed a modal strain energy method to identify both damage location and extent. Tian et al [14] used Uniform Load Surface (ULS) curvature to identify the delamination defects of the lattice sandwich plate. Zhu et al. [15] utilizes the frequency response function (FRF) measured at one point for damage identification of honeycomb sandwich beam. In the method, genetic algorithm is used to inverse damage features (location and extent). For

composite sandwich structures with honeycomb-core, Andrzej [16] proposed a novel approach of two-steps damage detection method based on wavelet transform. By using ULS, a baseline-free method is developed to determine the debonding of truss bar in composite lattice truss core sandwich structures [17]. Lu et al [18] proposed a damage identification method based on flexibility matrix for pyramidal SPTCs. Based on the method, an improvement was made to identify unbound nodes damages [19]. Seguel et al [20] used a high-speed 3D DIC system to assess the debonding of an aluminum honeycomb sandwich panel.

According to previous works, it is found that higher order modes are more sensitive to damage than lower order modes [21-22]. However, in the practical dynamic experiments, it is difficult to obtain higher order modes dues to the restrains of excitations and boundary condition. The limited structural modal information restricts effectiveness of vibration mode-based methods. Besides, the traditional methods are based on linear models of structures. Recently, some works have been conducted to investigate damage identification methods utilizing time series of structural responses [23-24]. Compared with vibration modes, it is easier to obtain structural time domain dynamic responses, which contains rich information. Manoach et al [25-27] has conducted a series of studies on damage detection of plates and composite beams by using time series analysis. Displacements and velocity responses are combined directly to construct damage indexes. Although an effective method contains plenty of information, the constructed expression may contradict to conventional cognition. It is more reasonable to combine or compare parameters in the same dimension.

In the present study, a damage identification method based on dimensionless time domain dynamic response is proposed for metallic SPTCs. Unlike previous works [25-

27], the proposed damage index is based on the combination of dimensionless displacement and velocity responses, and Teager energy operator (TEO) is also employed. Applications of the proposed method on metallic pyramidal SPTC with single damage and multiple damages are conducted. Effect of TEO on the effectiveness of the method is analyzed. Moreover, influences of some factors are discussed, including excitation force location, excitation frequency, boundary condition and number of points N in Poincare maps.

2. Damage detection technique

The proposed method is based on analyzing the Poincare maps, which contain data for displacements and velocities of structures in a compact form. Damage index $DIND_i$ utilizing dimensionless structural dynamic responses is presented,

$$DIND_i = \sum_{t=1}^{N} \sqrt{\left(\overline{s}_{i,t}^{\mathrm{D}} - \overline{s}_{i,t}^{\mathrm{I}}\right)^2 + \left(\overline{v}_{i,t}^{\mathrm{D}} - \overline{v}_{i,t}^{\mathrm{I}}\right)^2} \tag{1}$$

where N is the total number of points on Poincare maps, and subscript t denotes the t-th point on Poincare maps. $\overline{s}_{i,t}^{\mathrm{D}}$, $\overline{s}_{i,t}^{\mathrm{I}}$ and $\overline{v}_{i,t}^{\mathrm{D}}$, $\overline{v}_{i,t}^{\mathrm{I}}$ are the i-th node's dimensionless displacement and velocity response of the damaged and intact SPTC model respectively, as provided in Eq. (2). Superscripts D and I denote damaged and intact SPTC model, respectively.

$$\begin{aligned}
\overline{s}_{i,t}^{\mathrm{D}} &= \frac{s_{i,t}^{\mathrm{D}} - s_{\min,t}^{\mathrm{D}}}{s_{\max,t}^{\mathrm{D}} - s_{\min,t}^{\mathrm{D}}} \\
\overline{v}_{i,t}^{\mathrm{D}} &= \frac{v_{i,t}^{\mathrm{D}} - v_{\min,t}^{\mathrm{D}}}{v_{\max,t}^{\mathrm{D}} - v_{\min,t}^{\mathrm{D}}} \\
\overline{s}_{i,t}^{\mathrm{I}} &= \frac{s_{i,t}^{\mathrm{I}} - s_{\min,t}^{\mathrm{I}}}{s_{\max,t}^{\mathrm{I}} - s_{\min,t}^{\mathrm{I}}} \\
\overline{v}_{i,t}^{\mathrm{I}} &= \frac{v_{i,t}^{\mathrm{I}} - v_{\min,t}^{\mathrm{I}}}{v_{\max,t}^{\mathrm{I}} - v_{\min,t}^{\mathrm{I}}}
\end{aligned} \tag{2}$$

where $s_{i,t}^{\mathrm{I}}$ and $v_{i,t}^{\mathrm{I}}$ are the *t*-th point's displacement and velocity of the *i*-th node for the intact SPTC model. For the *t*-th point on Poincare maps, $s_{\max,t}^{\mathrm{I}}$ and $s_{\min,t}^{\mathrm{I}}$, $v_{\max,t}^{\mathrm{I}}$ and $v_{\min,t}^{\mathrm{I}}$ are the maximum and minimum displacement and velocity values of the intact structural all nodes' responses, respectively. $s_{i,t}^{\mathrm{D}}$, $v_{i,t}^{\mathrm{D}}$, $s_{\max,t}^{\mathrm{D}}$, $s_{\min,t}^{\mathrm{D}}$, $v_{\max,t}^{\mathrm{D}}$, and $v_{\min,t}^{\mathrm{D}}$ are parameters of the damaged SPTC model.

To suppress the fluctuations and singularities caused by non-damage factors (boundary condition, noise, shaker, etc.), TEO is utilized. Teager energy for a generalized discrete signal *f(n)* is defined as

$$T(f) = f^2(n) - f(n+1)f(n-1) \tag{3}$$

The damage index $DIND_i^{TEO}$ for spatial sampling points can be expressed as Eq. (4).

$$DIND_i^{TEO} = DIND_i^2 - DIND_{i+1} \times DIND_{i-1} \tag{4}$$

For SPTC model, the damage index can be developed as follow,

$$DIND_{(k,j)}^{TEO} = \sqrt{\left(DIND_{(k,j)}^2 - DIND_{(k+1,j)} \times DIND_{(k-1,j)}\right)^2 + \left(DIND_{(k,j)}^2 - DIND_{(k,j+1)} \times DIND_{(k,j-1)}\right)^2} \tag{5}$$

3. The case study

3.1 Model information

To investigate effectiveness of the proposed method, the pyramidal SPTC model is used. The sketch of the SPTC model and the unit cell are as shown in Fig. 1. The dimension of the truss core includes h_c=8 mm, t_c=1 mm and θ=45°. The thickness of the face sheets is 1 mm. There are eleven units along the length and width direction of the panel, respectively.

The SPTC is made of stainless steel with Young's modulus of 200 GPa, Poisson

ratio of 0.3, and mass density of 7800 kg/m^3. The boundary condition for the SPTC is two sides clamped and two sides free (CCFF). Three cases, including single damage (named SD) and multiple damages of different extents (MD1 and MD2), are studied in the work. MD1 contains two damages, one-cell missing and half-cell missing; MD2 contains three damages, one-cell missing, half-cell missing and one-bar missing (or 1/4 cell missing). The damaged specimens are shown in Fig. 2. Period excitation force (the red point in Fig.2) is applied on the center of the SPTC model. The excitation frequency is set as 2000 Hz, which is close to the 1st natural frequency of SPTC model (Table 1). The amplitude of the harmonic loading is 1 N. Green points in Fig.2 (a) are selected to compose the Poincare maps.

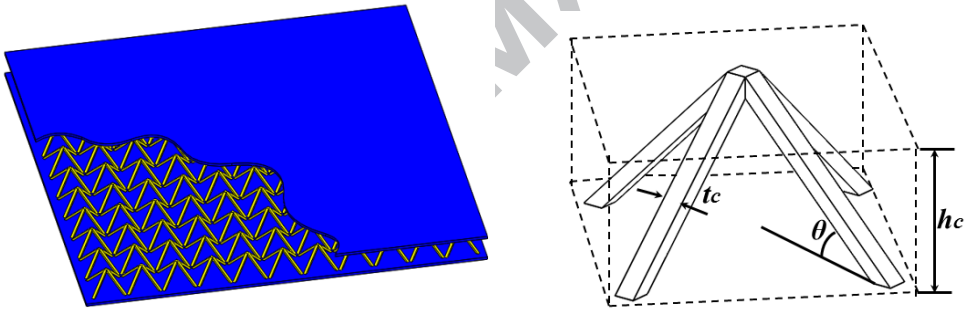

(a) **(b)**

Fig. 1 The model information. (a) Schematic of SPTC. (b) Unit cell of pyramidal truss.

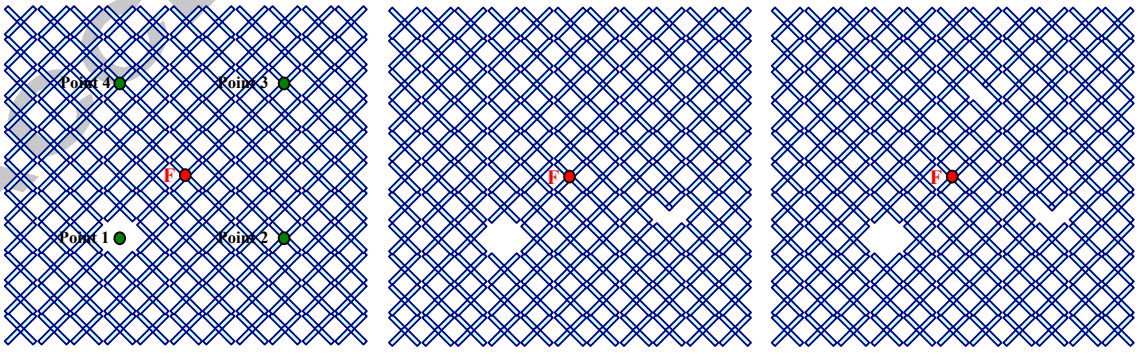

(a) **(b)** **(c)**

Fig. 2 Damaged SPTC models. (a) SD. (b) MD1. (c) MD2.

Table 1 Natural frequencies of the SPTC model

Mode order	Natural frequency (Hz)
1st	1872
2nd	2116
3rd	3651

3.2 Single damage identification

Influences of damage on the Poincare maps of four selected points (refer to Fig. 2 (a)) are presented in Fig. 3. From the left figures, it is seen that damages do not change the type of the Poincare section and only influence the length of the curves formed by the Poincare dots. After normalization, a new style of map is obtained, as the right figures of Fig. 3 shown. It is seen that the styles of curves formed by dots change a lot and damages change the locations of dots obviously. However, it is difficult to detect the real damage only according to the maps.

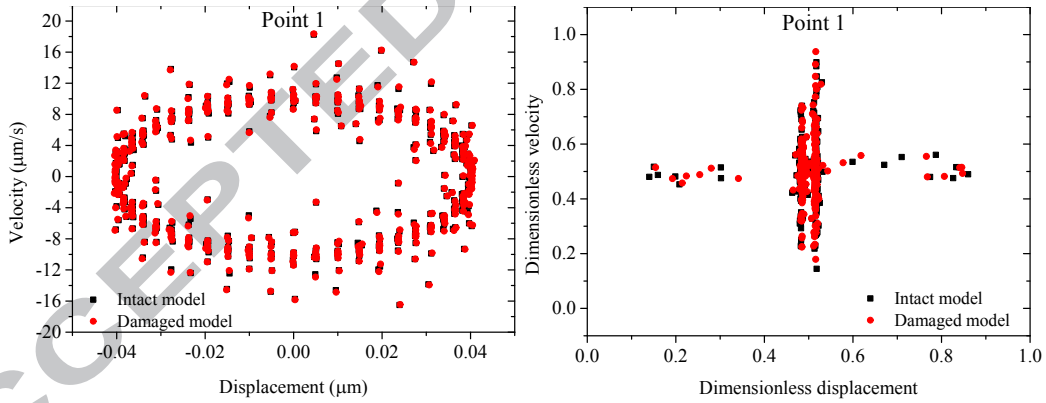

(a)

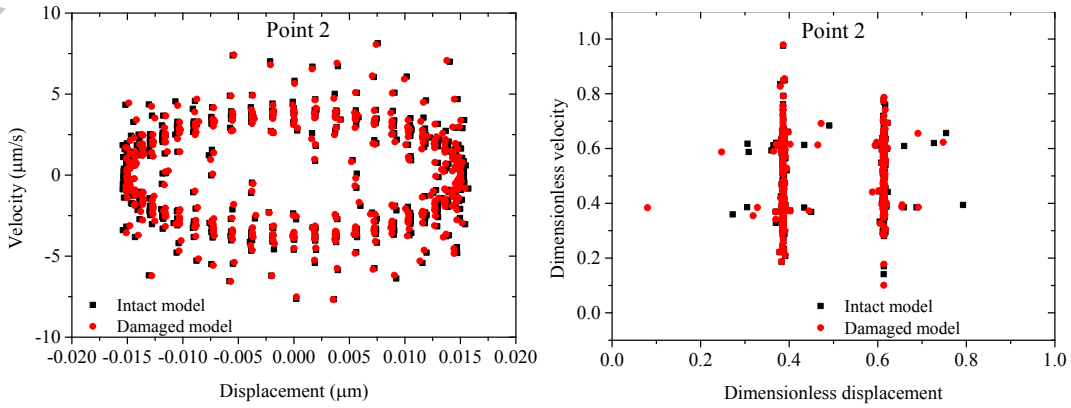

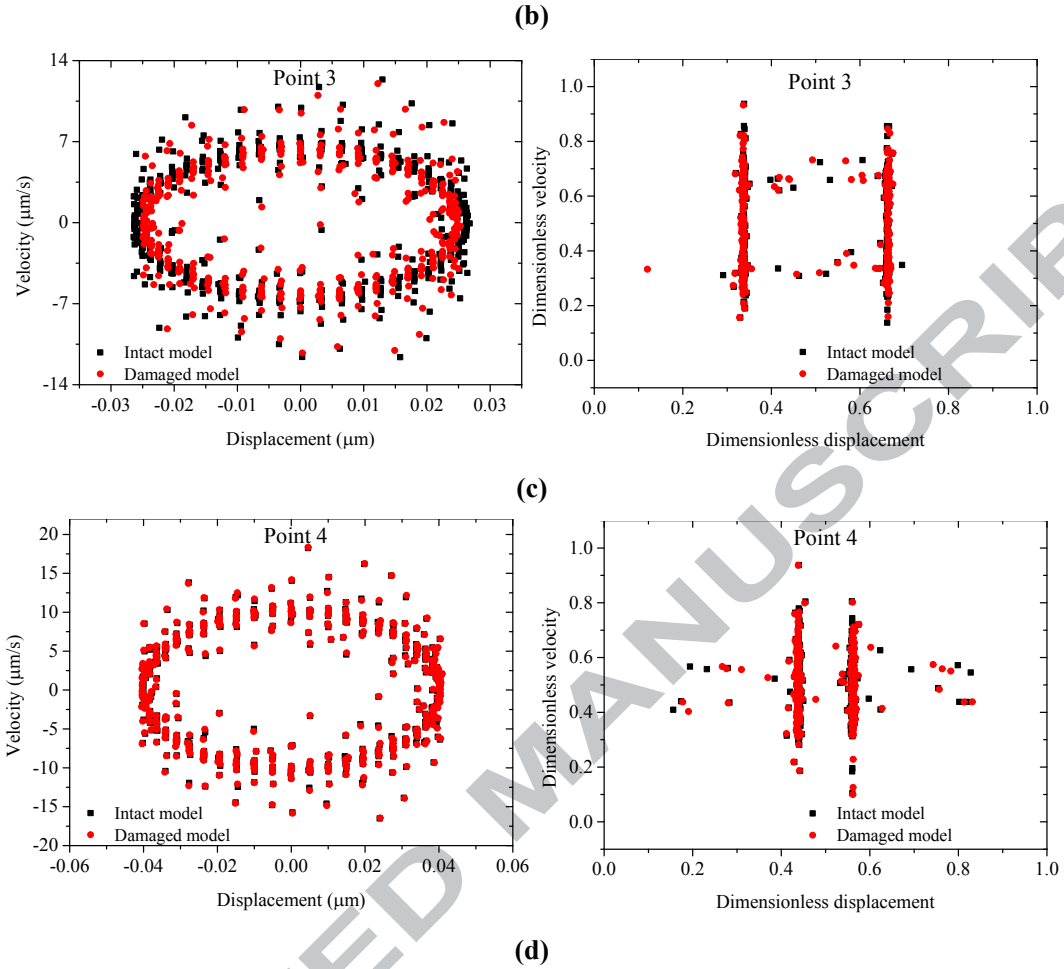

Fig. 3 Poincare maps based on the real responses and the dimensionless responses of (a) Point 1. (b) Point 2. (c) Point 3. (d) Point 4.

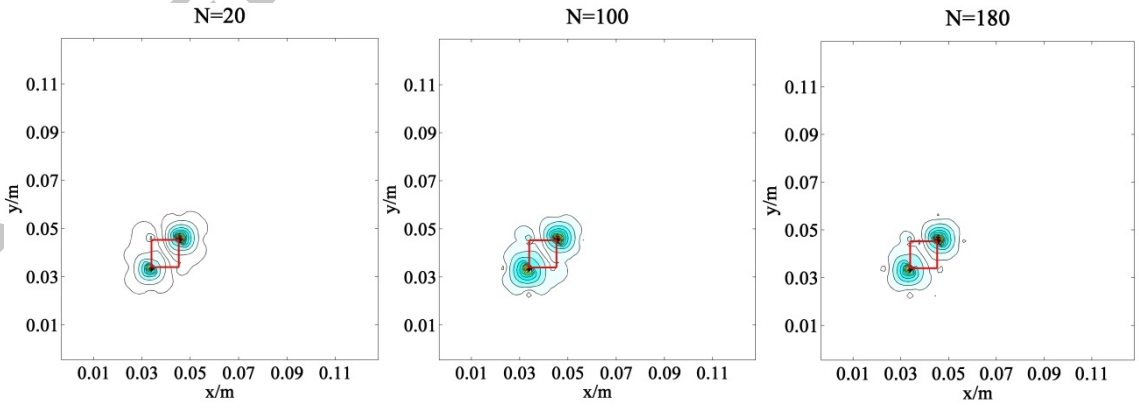

Fig. 4 Single damage identification.

Based on the structural dynamic responses, damage index $DIND_i^{TEO}$ is calculated. Results in the case of different N (N=20, N=100 and N=180) are provided in Fig. 4. In

Fig. 4, the red rectangle is the real location of damaged-cell. It is seen that zones with large $DIND_i^{TEO}$ value can predict the real damage location and the two points with largest damage index values can detect the beginning and ending locations of the damaged-cell accurately.

3.3 Multiple damages identification

Results of cases with multiple damages (Fig. 2 (b) and (c)) are presented in Fig. 5. From Fig. 5, it is seen that the proposed index $DIND_i^{TEO}$ can identify multiple damages with different extents effectively. Besides, in Fig.5, it is also found that contour plot features corresponding to different damage extents are different. For example, when only one area with high density of isograms arises at some local region, the corresponding damage is one-bar missing. When there are two areas with high density of isograms and the two areas are distributed parallel, the damage is half-cell missing. Further more, when the two areas are distributed diagonally, the damage is one cell missing. According to the results, it reveals that the proposed method can identify both structural damage locations and extents accurately.

From Fig. 5, it is also found that the figures would change a little as N increases from 20 to 180. In Fig. 5 (b), when N is 20 or 100, the accuracy of real damage identification is affected by fluctuations or noise around one-bar missing location. As N increases to 180, only the three damage locations are identified without any influence factors. The results demonstrate that parameter N could influence the effectiveness of the proposed method, which is discussed in Section 5.4.

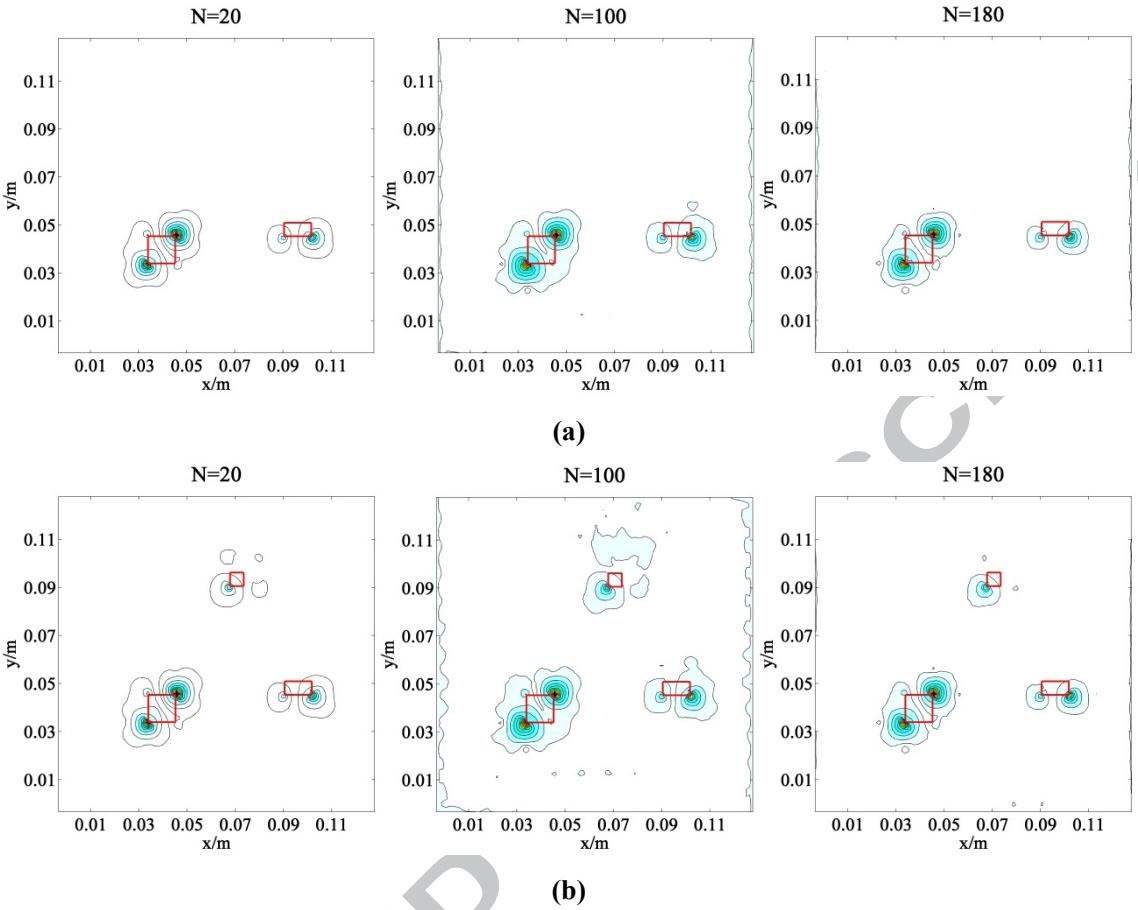

Fig. 5 Multiple damages identification. (a) MD1. (b) MD2.

3.3 Effect of TEO

To verify effectiveness of TEO on damage identification of SPTCs, results of $DIND_i$ for the cases SD, MD1 and MD2 are provided in Fig. 6. From Fig. 6, when TEO is not used to process the proposed damage index, there are fluctuations at the free boundary edges, which influence the identification of real damages. Especially when there are multiple damages with different extents, some undamaged zones with large index values or high density of isograms may arise. This causes a false damage identification. Comparing with results in Fig. 4 and Fig. 5, the fluctuations caused by boundary condition or environment can be effectively eliminated by processing $DIND_i$ with TEO.

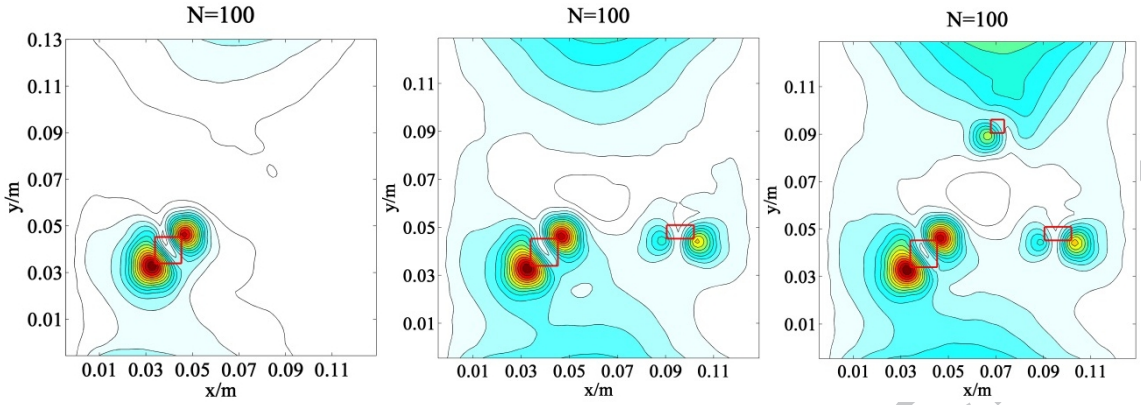

(a) **(b)** **(c)**

Fig. 6 Results of $DIND_i$. (a) SD. (b) MD1. (c) MD2.

4. Experimental validation

In the section, dynamic experiments of SPTCs are conducted to validate the effectiveness of the present method.

4.1 Experimental setup

In the experiment, the specimens are excited by a vibrator (JZK-50). The experimental setup is shown in Fig. 7(a). The excitation signal is generated by a laser Doppler vibrometer (Polytec, PSV-400) and amplified by a power amplifier (YE5874A) before inputted to the shaker. The excitation signal is sine and the corresponding frequency is 400 Hz. The sample frequency is 4000 Hz. The laser Doppler vibrometer is used to measure the structural dynamic response and the scanning points are placed on the front surface of the face sheet.

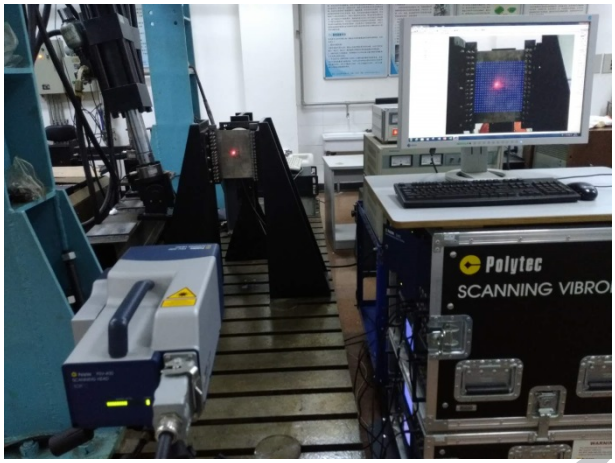

(a)

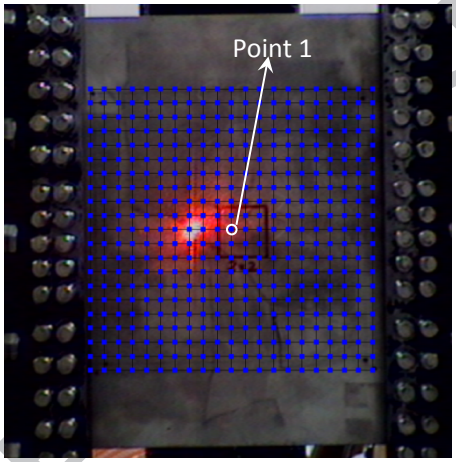

(b)

Fig. 7 Experimental setup. (a) Experimental setup. (b) Scanning points.

In the experiments, metallic pyramidal truss cores with a relative density ρ of about 3% are fabricated from 0.7 mm thick perforated stainless steel sheet by folding technique. The thickness of face sheet is 0.9 mm and the height of the truss core is 7 mm. The dimension of the metallic SPTC specimen is 250 mm×250 mm, and there are 22 cells in the row and 15 cells in the column.

In the study, cell missing damage is used to simulate structural damage. The truss core cells at the damage location are cut out before brazing. In the work, 2×3 cell missing is used and the red rectangle in Fig. 7 (b) is the 2×3 cell missing location.

To compare the dynamic response of damaged and intact specimens, the same

boundary condition and the excitation are applied on both damaged and intact specimens. During the measurement process, both the structural displacement and velocity responses are measured.

4.2 Experimental results

The displacement and velocity responses of Point 1 (in Fig. 7 (b)) are shown in Fig. 8(a). It is seen that damages do not change the type of the Poincare section and only influence the length of the curves formed by the Poincare dots. The experimental result is in accordance with the numerical results in Section 3.2. After normalization, the dimensionless dynamic responses are obtained and shown in Fig. 8(b). It is seen that the styles of curves formed by dots change a lot and damages change the locations of dots obviously.

Based on the dimensionless displacement and velocity, the damage index $DIND_i^{TEO}$ results in the case of the first 5, 10, 20 and 30 exciting periods are obtained, as shown in Fig. 9. From Fig. 9, it is seen that the cell missing damages can be identified by the proposed method effectively. As the number of exciting period increases, fluctuations caused by influence factors decreases and the improvement of the identification results increases obviously. Because the signal of structural dynamic response would strengthen and fluctuations caused by noise and other influence factors tend to be offset as the number of exciting period increases. The results demonstrate that parameter N could influence the effectiveness of the proposed method. The conclusion is in accordance with that in Section 3.3.

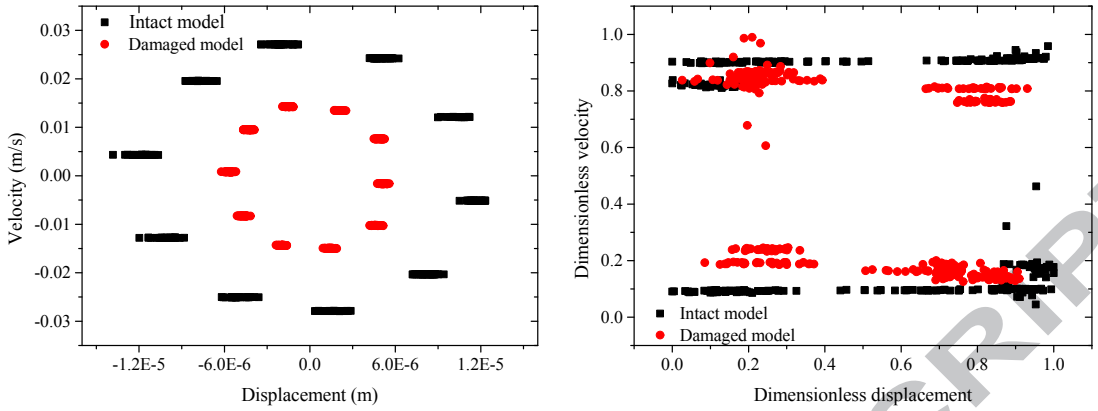

(a) (b)

Fig. 8 Dynamic response of Point 1. (a) Real responses. (b) Dimensionless responses.

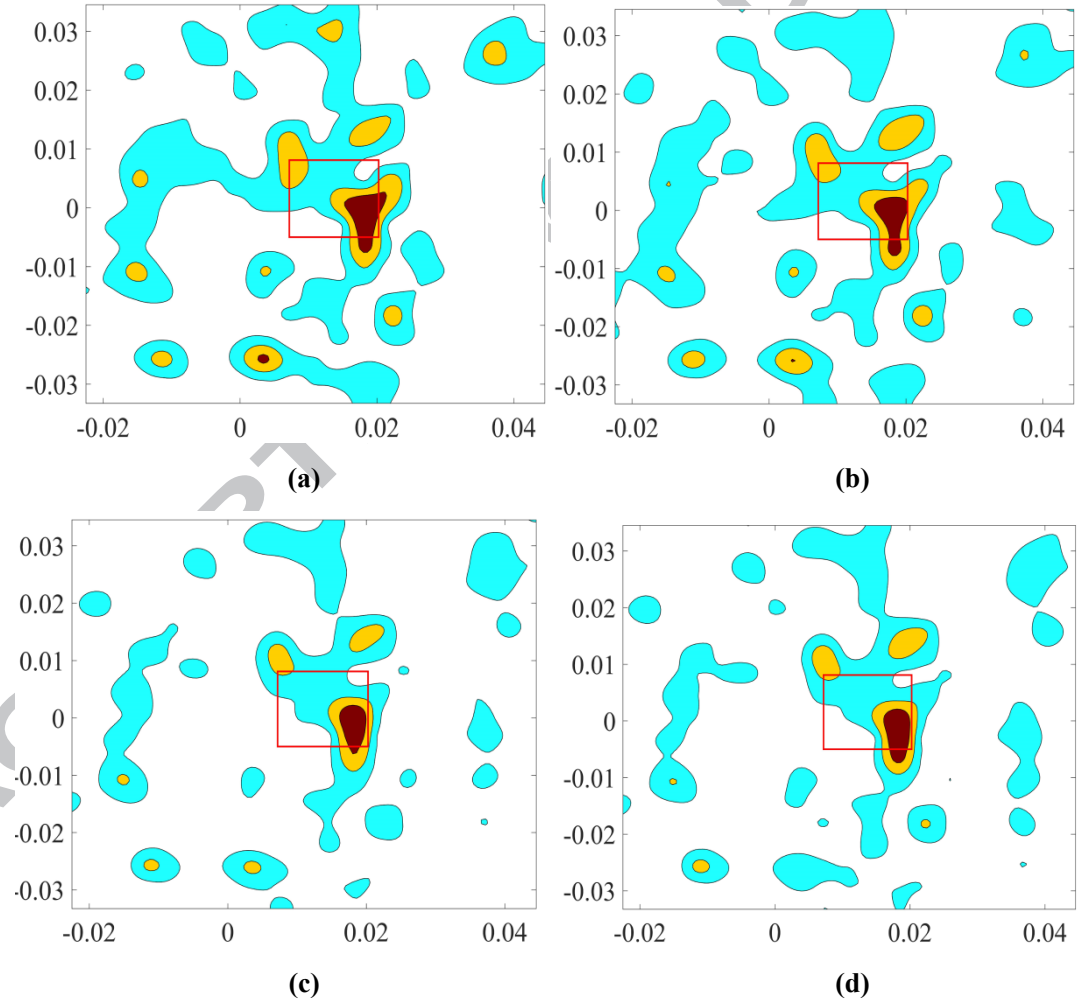

(a) (b) (c) (d)

Fig. 9 Dynamic response of point 1. (a) 5 exciting periods. (b) 10 exciting periods. (c) 20 exciting periods. (d) 30 exciting periods.

5. Discussions

The proposed method is based on structural time domain dynamic responses. Therefore any factors inflecting structural dynamic responses, would affect the effectiveness of the method, such as excitation location, excitation frequency and boundary condition. Besides, as Section 3.3 mentioned, parameter *N* may also affect the identification results.

5.1 Effect of excitation location

To investigate effect of excitation location, four other excitation locations are applied on SD1 model. Results are applied in Fig. 10, and the red "*" in the black circle indicates the excitation location.

In Fig. 10, when the excitation force is at Loc 1 or Loc 2, the one-cell missing damage could not be identified. This may attribute to a relatively long distance between the excitation force and damage location, and it is hard to excite the local vibration of the damage location. Therefore variations of structural responses caused by excitation are larger than those caused by damages, and the real damages are covered and cannot be identified. When the excitation force is near the damage (Fig. 10(c)), it is seen that the damage can be captured. Compared with results in Fig. 10(c), Fig. 4 and Fig. 5, the contour map is different, although the damage extent and location are same. The contour map in Fig. 10(d) can identify damage extent better. Those differences are caused by the excitation location.

According to Fig. 10, it reveals that excitation location plays a very important role on effectiveness of the proposed method. When the excitation is near the damage location or at some proper location in a distance, the damage can be identified more accurately. When excitation is far away from damage, damage may be covered by variation caused by other factors. Therefore, when applying the excitation force on

structures, several excitation locations can be tried in order to identify all the damages.

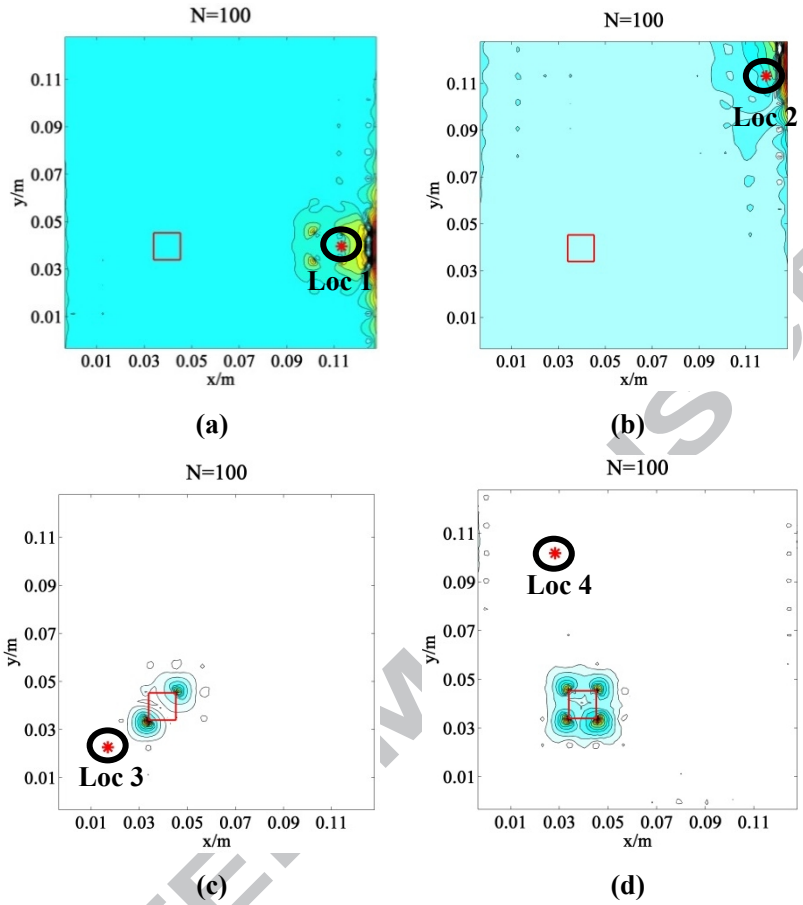

Fig. 10 Effect of excitation location. (a) Loc 1. (b) Loc 2. (c) Loc 3. (d) Loc 4.

5.2 Effect of excitation frequency

To study influence of excitation frequency, two types of excitation frequencies are selected: (a) excitation frequency equal (or close) to some order of natural frequency and (b) excitation frequency far away from any natural frequencies. In the study, six different excitation frequencies are used, including 400 Hz, 1000 Hz, 1870 Hz, 2800 Hz, 3500 Hz and 3650 Hz. According to Table 1, 400 Hz, 1000 Hz and 2800 Hz belong to type (b), and 1870 Hz, 3500 Hz and 3650 Hz belong to type (a). Moreover, 1870 Hz and 3650 Hz equal to the 1st and 3rd natural frequency respectively, and 3500 Hz is close to the 3rd natural frequency. Results are presented in Fig. 11.

From Fig. 11, the three damages can be detected no matter which excitation

frequency is employed, although there are different levels of noises. The noises in the cases with excitation frequency 1000 Hz and 3650 Hz are especially obvious; however, the damages can still be captured. It reveals that there is a great selection space of excitation frequencies for the proposed method.

Compared Fig. 11 (a) and (d) with other four figures, when the excitation frequencies are far away from structural natural frequencies, identification results are better than those cases with excitation frequencies equal or close to structural natural frequencies. In contrast, in Fig. 11 (f), when the excitation frequency equals to 3rd natural frequency, identification of one-bar missing is affected in some extent. It demonstrates that excitation frequencies equal to natural frequencies are not the best choice in some cases.

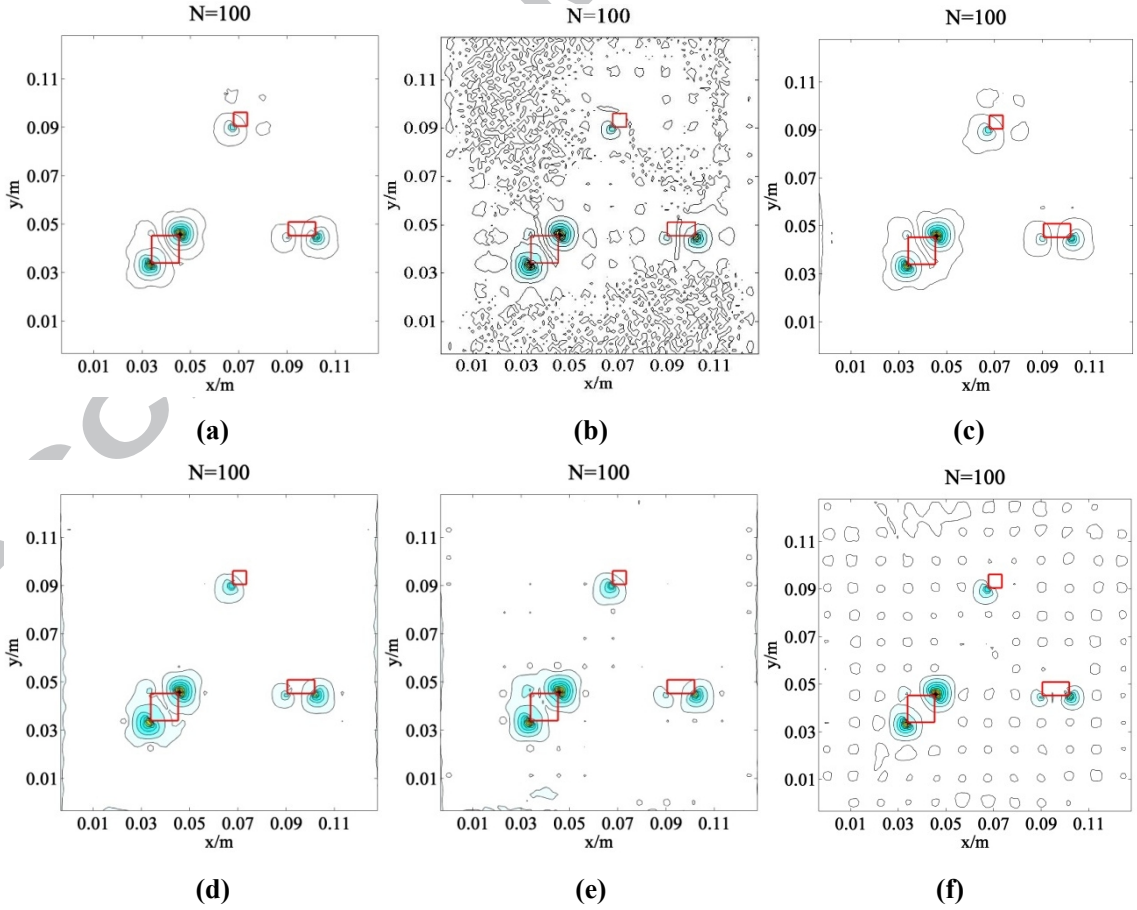

Fig. 11 Effect of excitation frequency. (a) 400 Hz. (b) 1000 Hz. (c) 1870 Hz. (d) 2800 Hz. (e)

3500 Hz. (f) 3650 Hz.

5.3 Effect of boundary condition

Two other boundary conditions are applied to investigate influence of boundary condition on the proposed method, including one side clamped and three sides free (CFFF) and fully clamped (CCCC). Results of SD and MD2 models are provided in Fig. 9.

From Fig. 12 (a1) and (b1), when boundary condition is CFFF, fluctuations or singularities caused by boundary condition and excitation are so large that they affect the identification of real damages. Especially, for the case of multiple damages, small extent damages, including half-cell missing and one-bar missing, are covered and cannot be detected. According to results in Fig. 4, Fig. 5 (b), Fig. 12 (a2) and (b2), as the restraint of boundary condition increases from CFFF to CCFF or CCCC, the single damage or multiple damages with different extents can be all identified effectively. When the constraint of boundary condition increases, complicated dynamic responses arise and local vibration modes appear, which are normally more sensitive to structural damages. The conclusion is in accordance with the previous studies [21-22].

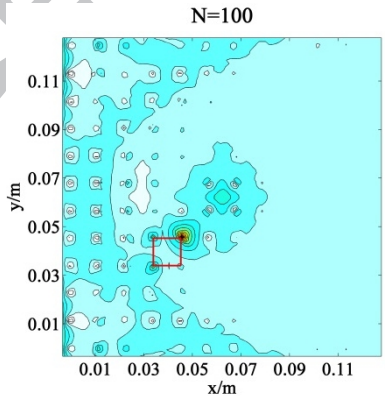

(a1)

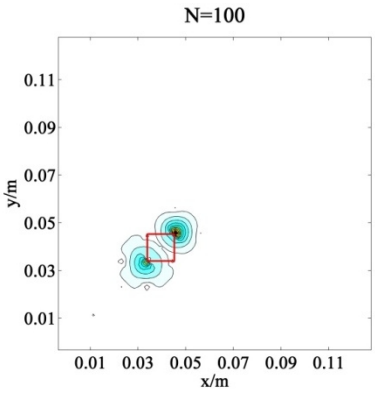

(a2)

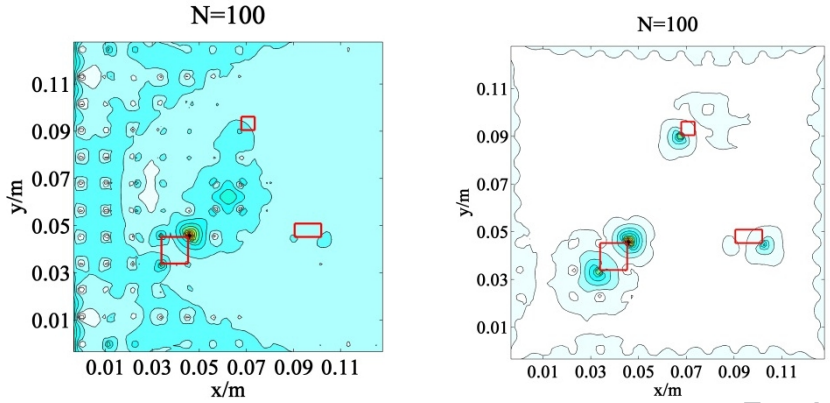

(b1) **(b2)**

Fig. 12 Effect of boundary condition. (a1) and (a2) are results of SD model in the case of CFFF and CCCC. (b1) and (b2) are results of MD2 model in the case of CFFF and CCCC.

5.4 Effect of parameter N

Results in the case of different parameters *N* for SD and MD2 are provided in Fig. 13. In Fig. 13, as the parameter *N* increases, many other influence factors arise and may cover the real damage. Especially, in Fig. 13(b), when *N* is 500, noises in red rectangles, which are caused by the restrained and free boundaries, are so large that small extent damage (one-bar missing) is diminished.

According to results in Fig. 5 (b), accuracy of the three damage identification increases as parameter *N* increases from 20 to 180. However, as *N* increases from 180 to 500, accuracy of damage identification decreases. It reveals that too large *N* is not beneficial for damage identification and proper parameter *N* value should be selected, in order to improve accuracy of the proposed method.

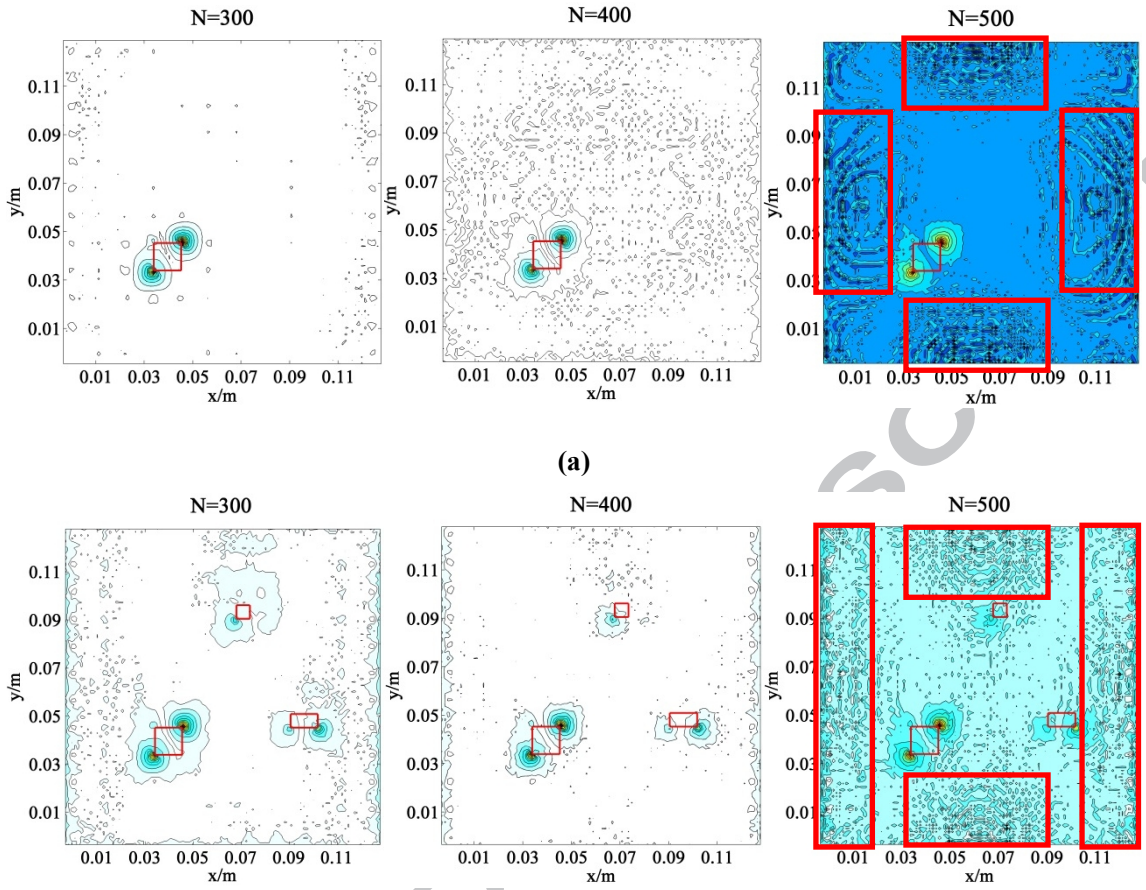

Fig. 13 Effect of parameter *N*. (a) SD. (b) MD2.

6. Conclusions

In the paper, a damage identification method based on the combination of dimensionless time domain dynamic responses and TEO is proposed for metallic SPTCs. Simulations of SPTC models with single and multiple damages are conducted. Experiments are conducted to verify the effectiveness of the proposed method. Effects of excitation location, excitation frequency, boundary condition, parameter N are analyzed and discussed. Some conclusions are obtained:

The proposed damage index $DIND_i^{TEO}$ can identify both single damage and multiple damages with different extents.

Effect of excitation location on damage identification is significant. In the practical tests, several different excitation locations should be applied on the structures, in order

to identify all of the damages. Effect of excitation frequency on damage identification is not so obvious, and there is a great selection space of excitation frequencies for the proposed method.

As the restraint of boundary condition increases from CFFF to CCFF or CCCC, effectiveness of the proposed identification method improves.

As parameter *N* increase, accuracy of damage identification increases firstly, then deceases after some special value. Proper parameter *N* value should be selected

Acknowledgements

This research is supported by the National Natural Science Foundation of China (Grant Nos. 11472276, 11332011 and 11502268) and National Defense Basic Scientific Research Program of China (Grant No. JCKY2016130B009).

References

1. Evans AG, Hutchinson JW, Fleck NA, Ashby MF, Wadley HNG. The topological design of multifunctional cellular metals. *Prog Mater Sci* 2001; 46: 309-327.

2. Wang J, Lu TJ, Woodhouse J, Langley RS, Evans J. Sound transmission through lightweight double-leaf partitions: theoretical modeling. *J Sound Vib* 2005; 286(4-5): 817-847.

3. Zumpano G and Meo M. Damage detection in an aircraft foam sandwich panel using nonlinear elastic wave spectroscopy. *Comput Struct* 2008; 86: 483-490.

4. Panopoulou A, Loutas T, Roulias D, Fransen S, Kostopoulos V. Dynamic fiber Bragg gratings based health monitoring system of composite aerospace structures. *Acta Astronaut* 2011; 69: 445-457.

5. Yuan W, Wang X, Song HW, Huang CG. A theoretical analysis on the thermal buckling behavior of fully-clamped sandwich panels with truss cores. *J Thermal Stresses* 2014; 37: 1433-1448.

6. Yuan W, Song HW, Wang X, Huang CG. Experimental investigation on thermal buckling behavior of fully-clamped truss-core sandwich panels. *AIAA Journal* 2015; 53(4): 948-957.

7. Manoach E, Trendafilova I. Large amplitude vibrations and damage detection of rectangular plates. *J Sound Vib* 2008; 315: 591-606.

8. Zou Y, Tong L, Steven GP. Vibration based model-dependent damage (delamination) identification and health monitoring for composite structures – a review. *J Sound Vib* 2000; 230(2): 357-378.

9. Rizos PF, Aspragathos N, Dimarogonas AD. Identification of crack location and magnitude in a cantilevered beam from the vibration modes. *J Sound Vib* 1990; 138: 381-388.

10. Andreaus U, Casini P, Vestroni F. Frequency reduction in elastic beams due to a stable crack: numerical results compared with measured test data. *Eng Trans* 2003; 51(1): 1-16.

11. Andreaus U, Baragatti P. Fatigue crack growth, free vibrations and breathing crack detection of aluminium alloy and steel beams. *J Strain Anal Eng Des* 2009; 44(7): 595-608.

12. Hu HW, Wang BT, Lee CH, Su JS. Damage detection of surface cracks in composite laminates using modal analysis and strain energy method. *Compos Struct* 2006; 74: 399-405.

13. Kumar M, Shenoi RA and Cox SJ. Experimental validation of modal strain energies

based damage identification method for a composite sandwich beam. *Compos Sci Technol* 2009; 69: 1635-1643.

14. Tian SX, Chen ZM, Chen LL, Zhang ZL. Numerical analyses on influence of damage configuration on vibration parameters for lattice sandwich plate. *Int J Appl Electrom* 2010; 33: 1565-1572.

15. Zhu KG, Chen MJ, Lu QH, Wang B, Fang DN. Debonding detection of honeycomb sandwich structures using frequency response functions. *J Sound Vib* 2014; 333: 5299-5311.

16. Andrzej K. Vibration-based spatial damage identification in honeycomb-core sandwich composite structures using wavelet analysis. *Compos Struct* 2014; 118: 385-391.

17. Li B, Li Z, Zhou J, Ye L, Li E. Damage localization in composite lattice truss core sandwich structures based on vibration characteristics. *Compos Struct* 2015; 126: 34-51.

18. Lu LL, Song HW, Yuan W, Huang CG. Baseline-free damage identification of metallic sandwich panels with truss core based on vibration characteristics. *Struct Health Monit*, 2017; 16(1):24-38.

19. Lu LL, Song HW, Huang CG. Experimental investigation of unbound nodes identification for metallic sandwich panels with truss core. *Compos Struct* 2017; 163: 248-256

20. Seguel F, Meruane V. Damage assessment in a sandwich panel based on full-field vibration measurements. *J Sound Vib* 2018; 417: 1-18.

21. Lu LL, Song HW, Huang CG. Effects of random damages on dynamic behavior of metallic sandwich panel with truss core. *Compos Part B-ENG* 2017; 116: 278-290.

22. Lou J, Wu LZ, Ma L, Xiong J, Wang B. Effects of local damage on vibration

characteristics of composite pyramidal truss core sandwich structure. *Compos Part B* 2014; 62: 73-87.

23. Cattarius J, Inman DJ. Time domain analysis for damage detection in smart structures. *Mech Syst Signal Process* 1997; 11: 409-423.

24. Moniz L, Nichols JM, Nichols CJ, Seaver M, Trickey ST, Todd MD, et al. A multivariate, attractor-based approach to structural health monitoring. *J Sound Vib* 2005; 283: 295-310.

25. Trendafilova I, Manoach E. Vibration-based damage detection in plates by using time series analysis. *Mech Syst Signal Process* 2008; 22: 1092-1106.

26. Manoach E, Samborski S, Mitura A, Warminski J. Vibration based damage detection in composite beams under temperature variations using Poincare map. *Int J Mech Sci* 2012; 62: 120-132.

27. Manoach E, Warminski J, Kloda L, Mitura A. Numerical and experimental studies on vibration based methods for detection of damage in composite beams. *Compos Struct* 2017; 170: 26-39.